Inhibitory Effects of Calcitriol on the Growth of MCF-7 Breast Cancer Xenografts in Nude Mice: Selective Modulation of Aromatase Expression in vivo

**Srilatha Swami · Aruna V. Krishnan ·
Jennifer Y. Wang · Kristin Jensen · Lihong Peng ·
Megan A. Albertelli · David Feldman**

Abstract Calcitriol (1,25-dihydroxyvitamin D$_3$), the hormonally active metabolite of vitamin D, exerts many anticancer effects in breast cancer (BCa) cells. We have previously shown using cell culture models that calcitriol acts as a selective aromatase modulator (SAM) and inhibits estrogen synthesis and signaling in BCa cells. We have now examined calcitriol effects in vivo on aromatase expression, estrogen signaling, and tumor growth when used alone and in combination with aromatase inhibitors (AIs). In immunocompromised mice bearing MCF-7 xenografts, increasing doses of calcitriol exhibited significant tumor inhibitory effects (~50% to 70% decrease in tumor volume). At the suboptimal doses tested, anastrozole and letrozole also caused significant tumor shrinkage when used individually. Although the combinations of calcitriol and the AIs caused a statistically significant increase in tumor inhibition in comparison to the single agents, the cooperative interaction between these agents appeared to be minimal at the doses tested. Calcitriol decreased aromatase expression in the xenograft tumors. Importantly, calcitriol also acted as a SAM in the mouse, decreasing aromatase expression in the mammary adipose tissue, while increasing it in bone marrow cells and not altering it in the ovaries and uteri. As a result, calcitriol significantly reduced estrogen levels in the xenograft tumors and surrounding breast adipose tissue. In addition, calcitriol inhibited estrogen signaling by decreasing tumor ERα levels. Changes in tumor gene expression revealed the suppressive effects of calcitriol on inflammatory and growth signaling pathways and demonstrated cooperative interactions between calcitriol and AIs to modulate gene expression. We hypothesize that cumulatively these calcitriol actions would contribute to a beneficial effect when calcitriol is combined with an AI in the treatment of BCa.

Keywords Calcitriol · Selective aromatase modulator · Estrogen synthesis · Aromatase · Aromatase inhibitors · Breast cancer · Xenografts

S. Swami · A. V. Krishnan · J. Y. Wang · L. Peng ·
D. Feldman (✉)
Department of Medicine–Endocrinology,
Stanford University School of Medicine,
Room S025, 300 Pasteur Drive,
Stanford, CA 94305–5103, USA
e-mail: dfeldman@stanford.edu

K. Jensen
Department of Pathology,
Stanford University School of Medicine,
Stanford, CA 94305, USA

K. Jensen
Department of Pathology,
Palo Alto Veterans Affairs Hospital Care Systems,
Palo Alto, CA 94304, USA

M. A. Albertelli
Department of Comparative Medicine,
Stanford University School of Medicine,
Stanford, CA 94305, USA

Introduction

Breast cancer (BCa) is the most common form of cancer in women in the United States. Approximately 70% of BCa are estrogen receptor positive (ER+) and are responsive to endocrine therapy. The hormonal drugs used to treat ER+ BCa are designed to antagonize the mitogenic effects of estrogens and include: selective estrogen receptor modulators (SERMs) such as tamoxifen and raloxifene that bind to the ER and act as antagonists in the breast; selective

estrogen receptor down-regulators (SERDs) such as fulvestrant that bind to and target ER for degradation; and aromatase inhibitors (AIs) that inhibit the activity of aromatase, the enzyme that catalyzes the synthesis of estrogens from androgenic precursors [1–3]. Currently, AIs are the first line therapy to prevent BCa progression in postmenopausal women following primary therapy [2, 4]. However, AI inhibition of aromatase is nonselective and occurs at all sites including bone, where normal estrogen function is required for the maintenance of bone mineralization. Thus prolonged therapy with AIs has the potential to lead to the undesirable side effect of osteoporosis [5, 6]. The development of agents that act as selective aromatase modulators (SAMs) inhibiting estrogen synthesis in the breast while allowing unimpaired estrogen synthesis in desirable sites such as bone would be clinically very useful [7].

Calcitriol (1,25-dihydroxyvitamin D_3), the hormonally active form of vitamin D exhibits antiproliferative and differentiation-inducing activities as well as inhibits tumor angiogenesis, invasion, and metastasis, suggesting its utility as an anticancer agent [8–13]. We have recently demonstrated that calcitriol acts as a SAM in cultured cells, decreasing aromatase expression in malignant breast epithelial cells and adipocytes while increasing aromatase expression in osteoblastic cells [14]. In addition, we and others have shown that calcitriol down-regulates the expression of ERα and thereby inhibits estrogen signaling in malignant breast epithelial cells [15–17]. Thus calcitriol is a potent inhibitor of both estrogen synthesis and signaling [18] and therefore has the potential to enhance the beneficial effects of both AIs and SERMs when combined with these drugs. Our earlier study demonstrated cooperative effects of calcitriol with three different AIs resulting in enhanced inhibition of BCa cell growth [14]. In the current study, we have examined the effects of calcitriol in vivo in nude mice bearing human BCa xenografts administered alone and in combination with AIs. Our goal was to determine whether calcitriol also acted as a SAM in vivo and reduced estrogen synthesis in the tumor microenvironment. Since calcitriol and the AIs act by different mechanisms to limit aromatase-mediated estrogen synthesis, we also investigated whether their combinations exhibited enhanced anticancer effects in vivo. Our results suggest that the use of calcitriol alone or in combination with AIs would have therapeutic utility in the treatment of ER+BCa.

Materials and Methods

Materials

Calcitriol, letrozole, and anastrozole were kind gifts from BioXell, Norvartis Pharma AG, and Astra Zeneca, respectively. Tissue culture media, supplements, and fetal calf serum (FCS) were obtained from Gibco BRL (Grand Island, NY), Lonza (Walkersville, MD), and Mediatech Inc. (Herndon, VA), respectively.

Methods

Cell Culture

MCF-7 human BCa cells were routinely cultured in DMEM/F12 medium containing 10% FBS at 37°C and 5% CO_2 in a humidified incubator. Before inoculation into nude mice, cell cultures were subjected to a screen to ensure the absence of murine viruses. Cultures grown to ~75% confluence in T-150 flasks were washed and digested with trypsin and cell pellets were obtained under sterile conditions. Cell pellets were resuspended (~10×10^7 cells/ml) in sterile culture media mixed with an equal volume of regular Matrigel (Collaborative Biomedical, Bedford, MA) prior to injections into mice.

Subcutaneous and Orthotopic Xenograft Establishment in Nude Mice

All animal procedures were performed in compliance with the guidelines approved by Stanford University Administrative Panels on Laboratory Animal Care (APLAC). Four- to 6-week-old female athymic, nude (Fox$_n$$^{nu/nu}$) intact, and ovariectomized (OVX) mice purchased from Harlan Laboratories (Indianapolis, IN) were housed in a designated pathogen-free area in the Research Animal Facility, Stanford University School of Medicine and fed irradiated mouse chow and autoclaved reverse osmosis-treated water. Xenografts were established in ~6-week-old mice by injections of MCF-7 cells (~10 million) suspended in a small volume (~100 μl) of the culture medium–Matrigel mixture. For subcutaneous xenografts, cells were injected subcutaneously into two sites: one each in the right and left flanks of intact mice (premenopausal model). Prior to establishing orthotopic xenografts in OVX mice (postmenopausal model), 15 mg/90 day time-release androstenedione pellets (Innovative Research of America, Sarasota, FL) were implanted into the intrascapular space in these mice. A midline abdominal skin incision was then made to visualize the fourth mammary fat pad (inguinal glands) and tumor cells were injected into the fat pad on both the right and left sides. For gene expression studies, the fat pads of the #4 inguinal mammary glands ("tumor bearing" fat pad) were compared to the fat pads of the thoracic (glands # 2 and 3) mammary glands, which did not contain any tumors ("non-tumor bearing" fat pad). For pellet implantation and tumor cell injection into the mammary fat pads, mice were manipulated in surgical aseptic conditions under isoflurane anesthesia and received carprofen (5 mg/kg) for analgesia. Body weight and tumor

size were measured once a week. Tumor volumes were calculated from two tumor diameter measurements using a vernier caliper and using the formula: tumor volume= (length × width^2)/2 [19]. When the tumors reached ~70 mm^3 in size, the mice were assigned to different treatment groups and the treatments were continued over the following 4 weeks.

Treatments

Mice were assigned to the different treatment groups such that there was no statistically significant difference in tumor volumes between the experimental groups at the beginning of treatment. Stock solutions of calcitriol and the AIs were made in 100% ethanol and stored at −20°C. Appropriate dilutions were made in sterile saline and the desired concentrations of the drugs in a small volume (100 μl) of the sterile saline vehicle were administered as intraperitoneal (i.p.) injections. The mice in the control group received i.p. injections of 0.1% ethanol in sterile saline (vehicle). The dosage of calcitriol and the intermittent administration regimen were based on published observations [20–22]. Calcitriol was administered at 0.025, 0.05, and 0.1 μg doses three times a week (on Mondays, Wednesdays, and Fridays). Anastrozole was administered at 5 μg and letrozole at 2.5 μg 6 days a week (Monday through Saturday). In the case of mice receiving combination regimens, on the days they received both calcitriol and the AI, the drugs were combined in the same volume of the vehicle and administered as a single injection. Treatments were continued for 4 weeks. Body weights and tumor sizes were measured weekly throughout the treatment period. At the end of the study, 14 h after the final calcitriol injections, mice were euthanized according to APLAC guidelines using CO_2. Blood samples were collected by cardiac puncture while under CO_2 anesthesia causing exsanguinations and serum samples were obtained. Tumors and other tissues (ovaries, uteri, bone marrow, and tumor-bearing and non-tumor-bearing mammary fat pads) were harvested, cleaned, and snap frozen in liquid nitrogen for later analysis. Bone marrow was removed by flushing the marrow cavity of the femur with 5 ml of PBS using a syringe and the bone marrow cells were collected by centrifugation for analysis. Aliquots of the tumor tissue were fixed in formalin and embedded in paraffin for immunohistochemical analysis.

Analysis of mRNA Expression by Reverse Transcription and Real-Time PCR

Total RNA was isolated from tumor and other tissue samples following homogenization using the Trizol reagent (Invitrogen, Carlsbad, CA) as described [23]. Five micro-

grams of RNA were subjected to reverse transcription using the SuperScript III first strand synthesis kit (Invitrogen) and an oligo-d(T) primer as previously described [14]. Relative changes in mRNA levels were assessed by the comparative C_T (DDC_T) method as described [24]. The mRNA expressions of the genes of interest were normalized to either TATA box-binding protein (TBP) or glyceraldehyde-3-phosphate dehydrogenase (GAPDH) mRNA levels as described previously [23]. The primers used for the measurement of total aromatase mRNA in the human xenograft tumors and the various mouse tissues were as previously described [25, 26].

Measurement of Estrone (E_1) and Estradiol (E_2) Levels

Protein extracts from mammary fat and tumor tissues were prepared by homogenizing the tissues in a Tris–EDTA buffer containing high salt as described previously [27]. Aliquots of the tissue extracts were used to measure E_1 and E_2 levels using enzyme immuno assay kits (Cayman Chemical Company, Ann Arbor, MI) following the manufacturer's protocols. Protein concentration of the extracts were determined by the method described by Bradford [28].

Measurement of Serum Calcium Levels

Serum calcium levels were measured using the QuantiChrom calcium assay kit (BioAssay Systems, Hayward, CA) following the manufacturer's protocol.

Immunohistochemical Analysis

Tumor tissue was fixed in 10% neutral-buffered formalin and processed for immunohistochemical (IHC) studies as described previously [29]. Sections of 5-μm thickness were placed on positively charged glass slides and baked at 60°C for approximately 1 h in a standard histology oven (Fisher Scientific, Houston, TX). Antibodies to ERα (clone 1D5, 1:80, Dako, Carpinteria, CA) and aromatase (1:100 mouse antihuman cytochrome P450 aromatase antibody; AbDSerotec, Raleigh, NC) were applied per standard immunohistochemistry [29] practice using a Dako autostainer (Dako). In negative controls, primary antibodies were omitted and IgG was used instead. Slides were counterstained with hematoxylin and coverslipped. Scoring was based on both percentage scale and intensity. Staining intensity was scored on a scale of 0 to 3+ with 0 being negative; 1+, weakly positive; 2+, moderately positive; and 3+, strongly positive. Staining intensity was rated similarly based on average intensity over the tumor cell population. Percentage of cells staining was subjectively estimated from examination of many fields at high magnification (200–400X).

Statistical Analysis

Statistical analyses were performed using the GraphPad Prism 5 software (GraphPad Software, San Diego, CA). Data were evaluated by ANOVA with Scheffe's F-test as the post-hoc analysis.

Results

We established human BCa xenografts by subcutaneous injections of a mixture of ER+MCF-7 cells and matrigel into the flanks of intact nude mice (premenopausal model) as well as into the mammary fat pads of OVX mice (postmenopausal model). Since one of our goals was to investigate the effect of calcitriol on estrogen synthesis, we did not provide E_2 supplementation to the mice, although typically the growth of MCF-7 xenografts in mouse models is supported by E_2 supplementation. In OVX mice we implanted pellets of the estrogenic precursor androstenedione to ensure local estrogen synthesis in the breast environment by aromatase present in the tumor cells as well as the surrounding mammary adipocytes. The effects of calcitriol on tumor growth and estrogen synthesis and signaling were investigated both when used alone and in combination with the AIs anastrozole and letrozole in the pre- and postmenopausal models, respectively.

Effects of Calcitriol on Tumor Growth, Body Weight, and Serum Calcium in Intact Mice

In the intact mice, tumors in the flank grew to ~70 mm^3 in size by 6 weeks after tumor cell inoculation in the absence of estrogen supplementation. The effects of calcitriol at very low (VLC; 0.025 μg/mouse), low (LC; 0.05 μg/mouse), and high (HC; 0. μg/mouse) concentrations on tumor growth and body weight were examined over the next 4 weeks (Fig. 1a). In the control group that received vehicle injections, the tumors continued to grow over the next 4 weeks, albeit at a slightly slower rate compared to the initial growth rate, reaching a mean volume of ~90 mm^3 by week 10. In calcitriol-treated mice, decreases in tumor volumes were evident as early as 1 week after initiation of treatment. Tumor volumes continued to decline in the calcitriol-treated groups. At the end of 4 weeks of treatment the mean tumor volumes were significantly lower ($p<0.01$) in all the calcitiol-treated groups with the VLC, LC, and HC doses causing ~50%, ~60%, and ~70% reductions in mean tumor volumes compared to the control group. Compared to the VLC group, significantly greater tumor inhibition was achieved in the mice receiving HC ($p<0.05$ compared to VLC). There were no changes in the mean body weights between the experimental groups (Table 1),

suggesting that the doses of calcitriol used in the study were well tolerated by the mice. Measurement of serum calcium levels 14 h after the final calcitriol injections revealed no changes in the VLC group compared to control (Table 1). However small statistically significant increases were seen in mice receiving LC and HC (mean serum calcium levels at 10.9 ± 0.2 and 11 ± 0.3 mg/dl, respectively) compared to control (9.5 ± 0.3 mg/dl).
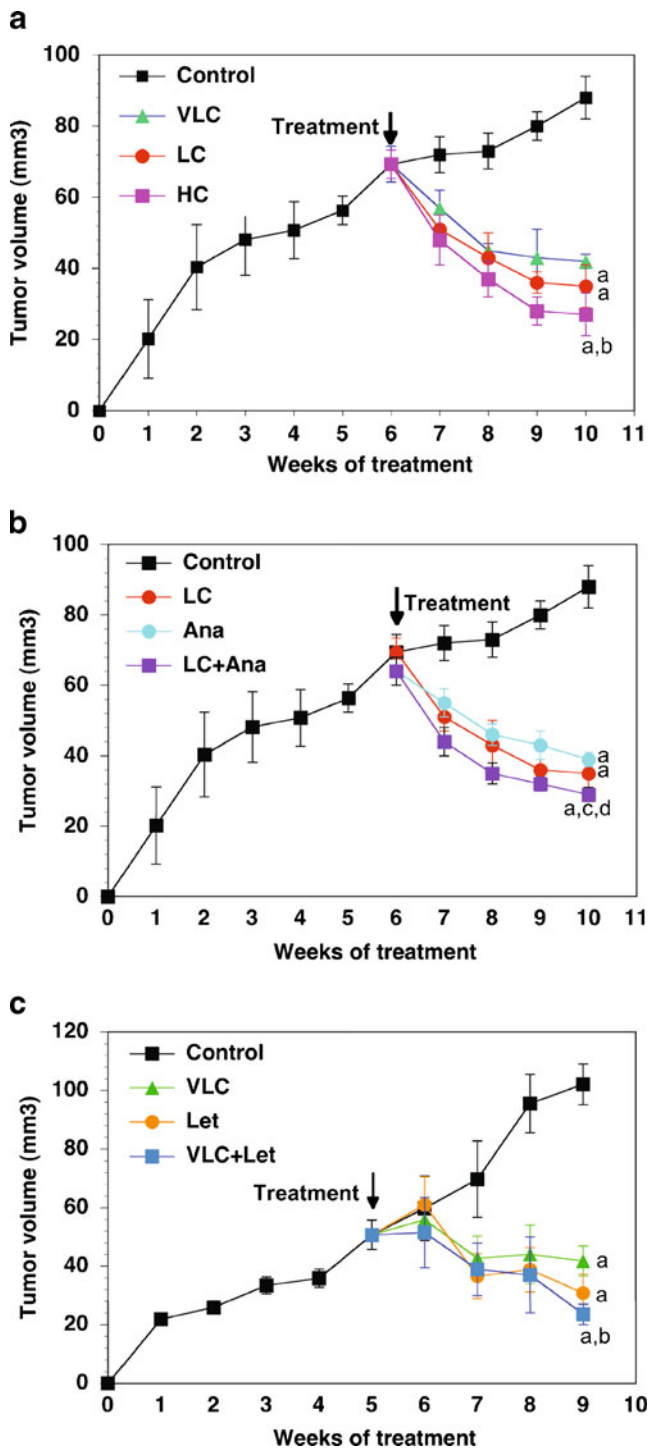
Effects of Calcitriol − AI Combinations on Tumor Growth, Body Weight, and Serum Calcium

The effects of the combinations of LC with the AI anastrozole at a suboptimal concentration (5 μg/mouse) were tested in the premenopausal model. Both LC and anastrozole were inhibitory to tumor growth. Decreases in tumor volume became obvious as early as 1 week after treatment with the decrease in the combination group attaining statistical significance ($p<0.01$) when compared to control (Fig. 1b). Tumor volumes in all the treated groups revealed significant decreases over time. At the end of 4 weeks of treatment the mean tumor volumes were significantly lower ($p<0.01$) in LC, anastrozole, and the combination groups compared to the control group with the tumor volume being the lowest in the combination group. Although the combination caused a small but statistically significant further decrease in mean tumor volume compared to LC alone or anastrozole alone ($p<0.05$) at the end of 4 weeks, the cooperativity between the two agents was minor. LC and anastrozole when combined at these doses caused no significant change in mean serum calcium levels or body weight (Table 1).

Similar data were obtained when the effect of a combination of VLC and the AI letrozole (at 2.5 μg/mouse) was tested on tumors growing in the mammary fat pads of OVX mice supplemented with androstenedione (postmenopausal model, Fig. 1c). At the end of 4 weeks of treatment the mean tumor volumes were significantly lower ($p<0.01$) in VLC, letrozole, and the combination groups compared to the control group. The mice receiving VLC–letrozole combination exhibited a further statistically significant decrease in mean tumor volume compared to VLC alone ($p<0.05$) but not when compared to letrozole alone. In the OVX mice the VLC dose did not significantly alter serum calcium levels or body weight (Table 1) when used alone or in combination with letrozole.

Tissue-Specific Regulation of Aromatase Expression by Calcitriol

Administration of LC to intact mice significantly decreased total aromatase mRNA in the xenografted human tumors (Fig. 2a; ~65% decrease). In the case of the various mouse tissues examined (Fig. 2a), LC caused a significant decrease in mammary fat aromatase mRNA levels. No

Fig. 1 Effect of calcitriol, AIs, and their combinations on the growth of MCF-7 tumors. MCF-7 xenografts were established in the flanks of intact nude mice (premenopausal model). After 6 weeks of tumor growth the mice were given i.p. injections of calcitriol at very low (*VLC*, 0.025 μg/mouse), low (*LC*, 0.05 μg/mouse), and high (*HC*, 0.1 μg/mouse) concentrations three times a week for the following 4 weeks. Tumor volumes were measured weekly and calculated as described in Materials and Methods (**a**). Some mice received anastrozole (*Ana*, 5 μg/mouse, s.c. or i.p. injections 6 days a week) as a single agent or in combination with LC (LC+Ana) and the tumor volumes were measured over the next 4 weeks (**b**). In separate experiments, MCF-7 xenografts were established in right and left fourth mammary fat pads of OVX nude mice (postmenopausal model) implanted with 60-day time-release androstenedione pellets and allowed to grow for 6 weeks. The mice received very low dose calcitriol (*VLC*, 0.025 μg/mouse, three times a week as i.p. injections), letrozole (*Let*, 2.5 μg/mouse, s.c. or i.p. injections 6 days a week) or a combination of both (VLC+Let) and the tumor volumes were measured over the next 4 weeks (**c**). Values represent mean±SE. Number of mice in the various experimental groups were as follows: In **a** and **b**, control=17, VLC=6, LC=10, HC=8, Ana=17, and LC+Ana=18. In **c**, control=13, VLC=6, Let=13, and VLC+Let=12. a=$p<0.001$ as compared to control, b=$p<0.05$ as compared to VLC, c=$p<0.05$ as compared to LC, and d=$p<0.05$ as compared to Ana

thoracic glands (~3-fold increase, $p<0.05$). VLC treatment significantly decreased aromatase mRNA expression seen in non tumor-bearing mammary fat tissue (~50% decrease, $p<0.05$) as well as in the mammary fat tissue surrounding the tumors, which exhibited elevated basal aromatase expression (~80% decrease due to VLC).

Changes in Tumor Gene Expression due to Calcitriol, AI, and Their Combinations

We next examined the effect of calcitriol when administered alone and in combination with an AI on tumor gene expression as a measure of its ability to inhibit estrogen synthesis (aromatase) and signaling (ERα) as well as to exert anti-inflammatory (COX-2) and antiproliferative (p21

Table 1 Serum calcium and body weight measurements

Groups	Body weight (gm)	Serum calcium (mg/dl)
Intact mice		
Control	22.0±0.4	9.5±0.3
VLC (0.025 μg)	23.6±0.7	9.8±0.6
LC (0.05 μg)	23.8±0.8	10.9±0.2*
HC (0.1 μg)	23.9±0.6	11.0±0.3*
Anastrozole (5 μg)	23.4±0.3	9.2±0.5
LC+Anastrozole	23.6±0.7	9.2±0.7
OVX mice		
Control	28.7±0.8	9.7±0.5
VLC (0.025 μg)	29.7±0.6	9.8±0.5
Letrozole (2.5 μg)	29.6±0.4	9.0±1.3
VLC+Letrozole	29.2±0.9	8.2±1.2

* $p<0.001$ when compared to control

changes in aromatase mRNA were seen in the ovaries and the uteri. In contrast, in bone marrow cells an approximately 4-fold increase in aromatase mRNA was seen due to LC administration.

As shown in Fig. 2b, in OVX mice, aromatase mRNA level was elevated in the tumor-bearing mammary fat tissue from the #4 inguinal glands when compared to fat tissue from non tumor-bearing fat pads from the # 2 and 3
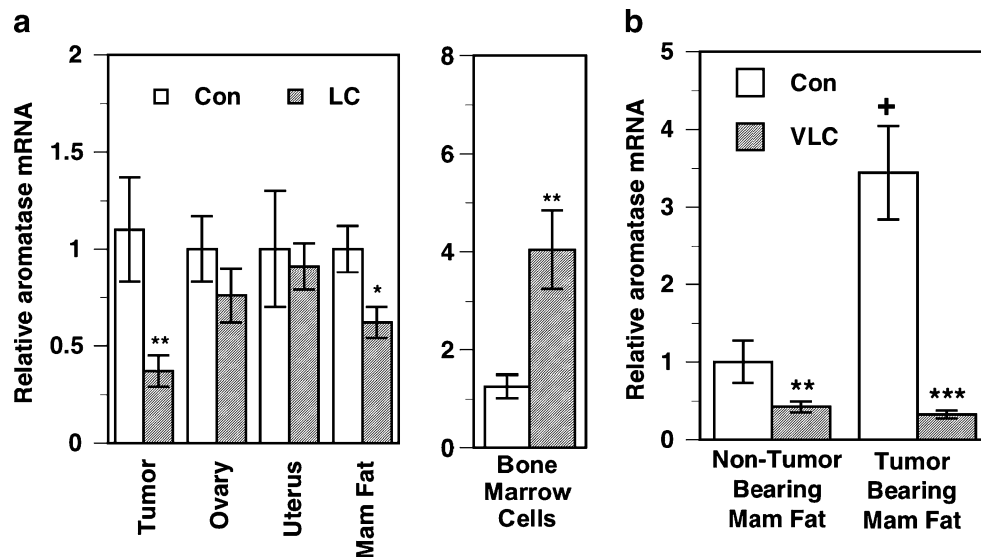
Fig. 2 Tissue-specific regulation of aromatase expression by calcitriol. (**a**) Total aromatase mRNA levels were measured by qRT-PCR as described in Materials and Methods in tumors, ovaries, uteri, mammary fat, and bone marrow cells from intact mice receiving low dose calcitriol (*LC*) treatment as described in Fig. 1. Relative aromatase mRNA levels in control mice was set at 1 for each tissue. Values represent mean±SE from six to 11 determinations. *$p < 0.05$ and **$p < 0.01$ as compared to control. (**b**) Total aromatase mRNA levels were measured in adipose tissue from non- tumor-bearing and tumor-bearing mammary fat pads from OVX mice receiving very low dose calcitriol (*VLC*) treatment as described in Fig. 1. Values represent mean±SE from 6 to 11 determinations. +$p < 0.05$ when the levels in tumor bearing adipose tissue in control mice were compared to the levels in non-tumor-bearing adipose tissue in control mice. **$p < 0.01$ when the levels in the non-tumor-bearing and tumor bearing mammary fat in mice receiving VLC were compared to the corresponding control mice receiving vehicle

and IGFBP-3) effects. As shown in Fig. 3a, LC administration resulted in significant decreases in tumor levels of ERα, aromatase and COX-2 mRNA levels as compared to control. Interestingly, anastrozole also significantly reduced aromatase and COX-2 mRNA, but not ERα mRNA levels. The combination treatment elicited maximal suppression of ERα, aromatase, and COX-2 mRNA expression in comparison to control. The suppressive effects of the combination on aromatase and COX-2 expression were significantly greater than those of the individual drugs on the expression of these genes ($p < 0.05$ for the effect of the combination vs. LC alone or anastrozole alone). In contrast, LC caused significant increases in p21 and IGFBP-3 mRNA levels as compared to control (Fig. 3b). The effects were again maximal in mice treated with the combination. Anastrozole alone did not significantly alter p21 and IGFBP-3 mRNA (Fig. 3b). Tumor gene expression analysis in OVX mice also produced similar results. The VLC-letrozole combination caused maximal decreases in ERα, aromatase and COX-2 mRNA (Fig. 3c). VLC by itself produced modest increases in tumor p21 and IGFBP-3 mRNA levels, while VLC–letrozole combination elicited maximal increases in the expression of these genes (Fig. 3d).

Figure 4 depicts changes in tumor ERα and aromatase protein expression due to LC, anastrozole, and their combination as determined by IHC analysis. The various treatments did not change the basic morphology of the tumors. The tumors were characterized as cohesive clusters and groups of cells with enlarged and mildly pleomorphic nuclei. Interspersed within the tumors were variable amounts of lymphocytes and some fibrous tissue. Nuclear ERα protein expression was maintained in all the treated tumors (Fig. 4a–d). A trend toward decreased percentage of cell staining was observed with calcitriol treatment and was most obvious in the tumors treated with the combination of LC and anastrozole (95% in the controls to 50% in the combination). Similarly, the intensity of staining also decreased from 3+ (strongly positive) to 2–3+ (moderately positive). Figure 4e–h depicts staining for aromatase protein expression. Ninety percent of the cells stained strongly for the expression of aromatase, which could be detected in both the cytoplasm and nuclei. Expression of aromatase decreased in all the treated tumors with the combination showing lower intensity (1+) than either calcitriol (2+) or anastrozole (2+) used individually. Overall, combination of LC with anastrozole resulted in lower protein expression of both ERα and aromatase in the tumors.

Effects of Calcitriol, Letrozole, and Their Combination on E_1 and E_2 Levels in Tumors and Surrounding Mammary Adipose Tissue

In the OVX mice receiving supplements of the estrogenic precursor andostenedione, we determined the effect of the

Fig. 3 Changes in tumor gene expression due to calcitriol, AI, and their combinations. Vehicle (control, *Con*), calcitriol, AIs, and their combinations were administered to tumor bearing intact (**a** and **b**) or OVX (**c** and **d**) mice as described in Fig. 1. Total RNA was isolated from harvested tumors and the mRNA levels of ERα, aromatase COX-2, p21, and IGFBP-3 were determined by qRT-PCR as described in Materials and Methods. Relative mRNA expression for each gene in tumors from control mice was set at 1. Values represent mean±SE from six to 11 determinations. $^{*}p<0.05$, $^{**}p<0.01$, and $^{***}p<0.001$ as compared to control. $^{+}p<0.05$ and $^{++}p<0.01$ as compared to LC or VLC. $^{\wedge}p<0.05$ and $^{\wedge\wedge}p<0.01$ as compared to Ana or Let
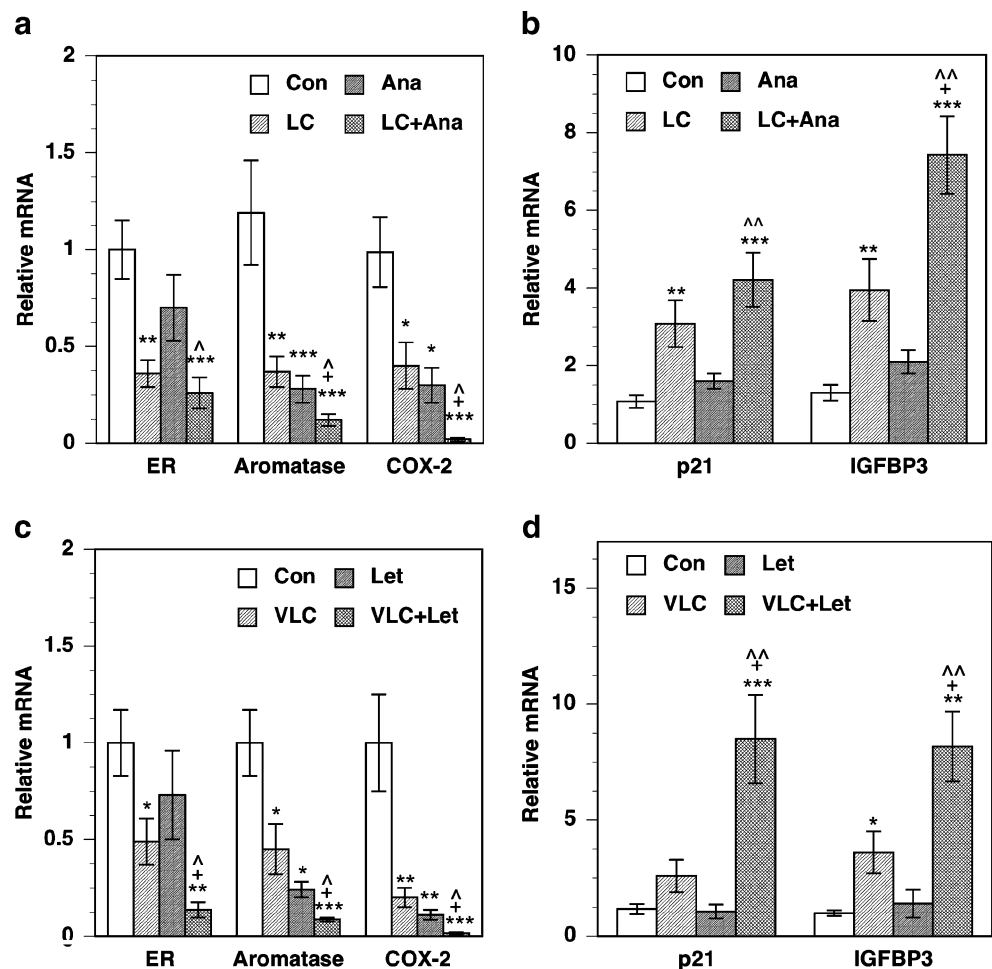

treatments on estrogen synthesis by measuring the levels of E_1 and E_2 both in the tumors and the surrounding mammary adipose tissue. We saw statistically significant decreases in E_2 levels due to treatments in tumors and the surrounding mammary adipose tissue compared to control (Fig. 5a). The combination treatment decreased tumor E_2 levels to an extent similar to that caused by calcitriol or letrozole when used individually. In tumor-surrounding mammary adipose tissue, however the combination elicited significantly greater reductions in E_2 levels compared to calcitriol alone ($p<0.05$) or letrozole alone ($p<0.01$). VLC and letrozole individually and in combination produced significant decreases in tumor E_1 levels compared to control (Fig. 5b). The combination treatment resulted in the lowest level of E_1 in the tumors, which was significantly lower than treatment with calcitriol alone ($p<0.05$). Changes in E_1 levels in the surrounding mammary adipose tissue reflected a similar decreasing trend following treatments with calcitriol or letrozole as single agents, which was not statistically significant. However, the decrease due to the combination treatment attained statistical significance (Fig. 5b).

In the tumors and the surrounding mammary fat we also measured the mRNA expression of 17β-hydroxysteroid dehydrogenase-1 (17β-HSD1), the reductive isoform of the enzyme that converts E_1 to E_2. However, we found no change in its expression following treatments (data not shown).

Discussion

Calcitriol and its analogs have been shown to exhibit antitumor effects in vivo in nude mice bearing xenografts of human BCa cells [30–33]. Several studies have demonstrated the requirement of sustained circulating levels of estrogens for the growth of MCF-7 tumors in OVX mice, which is provided by exogenous E_2 administration [32, 34, 35]. Since one of the main goals of this study was to investigate the effect of calcitriol and its combinations with AIs on estrogen synthesis in vivo, we did not provide E_2 supplementation to the mice. Tumor growth in the intact mice was dependent on their endogenous circulating estrogen levels. In the OVX mice, we implanted pellets releasing the estrogenic precursor androstenedione, which could then be converted locally (within the tumors and surrounding mammary adipose tissue) to E_1 by the aromatase present in these sites [36]
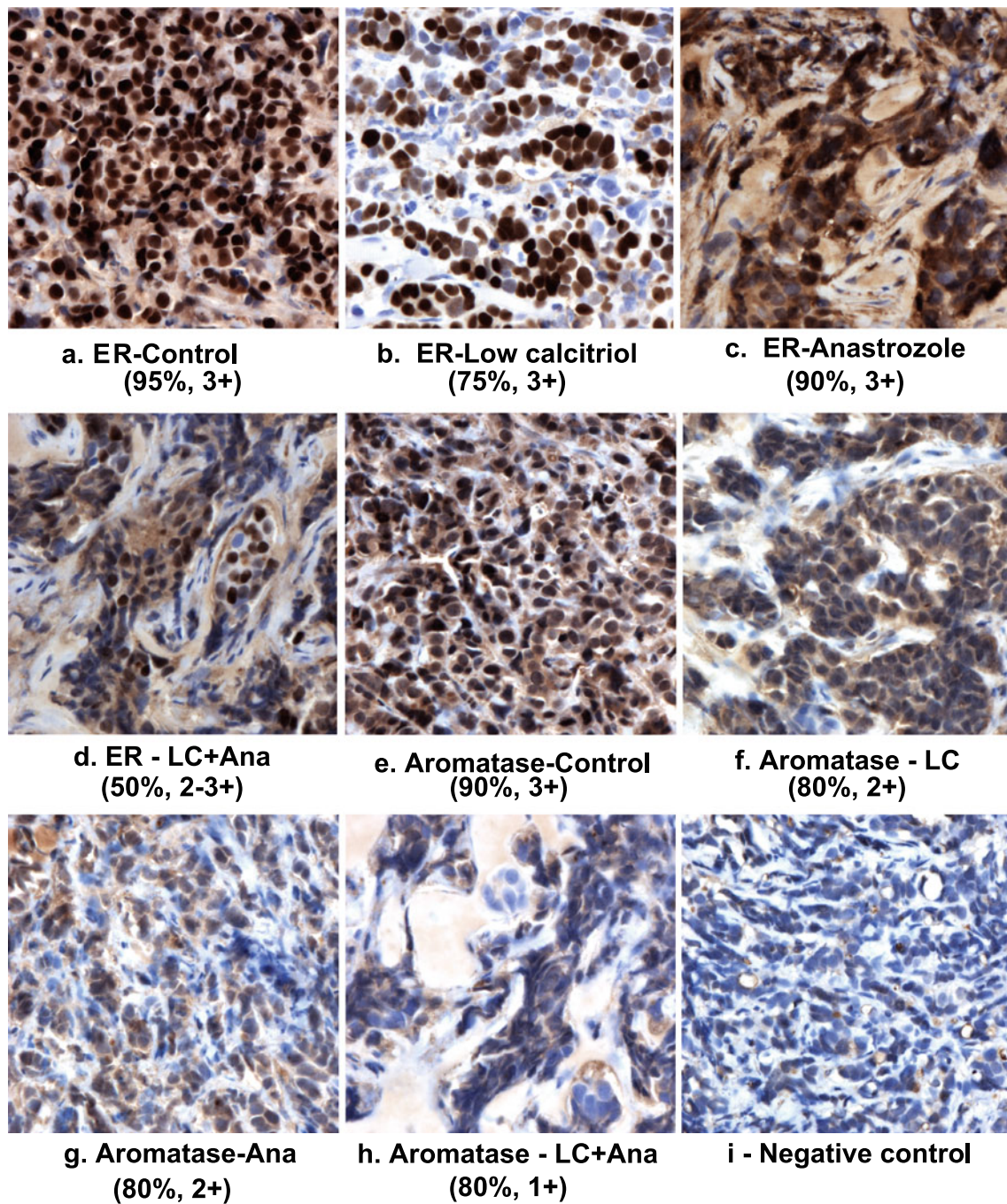
Fig. 4 Effect of calcitriol, anastrozole, and their combinations on ERα and aromatase protein expression in tumors. Vehicle (control, *Con*), low dose calcitriol (*LC*), anastrozole (*Ana*), and their combination (*LC+Ana*) were administered to intact mice as described in Fig. 1. Tumors were harvested and fixed for IHC analysis of aromatase and ERα expression as described in Materials and Methods. All tumors were immunostained with either anti-ERα antibody (**a–d**) or an anti-aromatase antibody (**e–h**) and are shown at 400× magnification. **i** Immunostaining with IgG (negative control). Numbers 0 to 3+ indicate the intensity of staining and numbers followed by the % sign indicate percentage of cells showing positive staining

and subsequently to E$_2$ by the activity of the enzyme 17β-HSD [37]. Therefore, in the absence of exogenously added estrogens, the tumor sizes in our mice were significantly less than reported tumor sizes in some studies where the mice received E$_2$ supplementation [30, 32, 33]. However, we did see a time-dependent increase in tumor growth although the growth rate showed a more pronounced increase in the first 6 weeks after tumor cell inoculation.

All three concentrations of calcitriol used in our study exerted significant tumor inhibitory effects and maximal
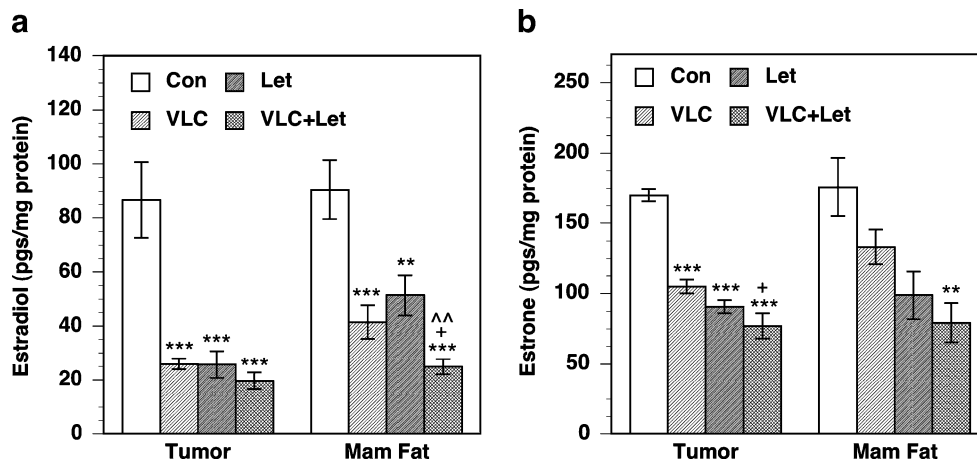
Fig. 5 Effects of calcitriol, letrozole, and their combination on E_2 and E_1 levels in tumors and surrounding mammary adipose tissue. Vehicle (control, *Con*), very low dose calcitriol (*VLC*), letrozole (*Let*), and their combination (*VLC+Let*) were administered to OVX mice as described in Fig. 1. Tumors and surrounding mammary adipose tissue were harvested from the mice and E_2 (**a**) and E_1 (**b**) levels in the tissue extracts were determined as described in Materials and Methods. Values represent mean±SE from five to 10 determinations. **$p < 0.01$ and ***$p < 0.001$ as compared to control. +$p < 0.05$ as compared to VLC. ^^$p < 0.01$ as compared to Let

inhibition was seen with the highest dose used (0.1 μg/mouse). We evaluated the toxicity of the treatments by monitoring body weights and serum calcium levels. No significant or irreversible weight loss occurred in any of the treatment groups. However, not unexpectedly, small statistically significant increases in serum calcium levels were seen in mice receiving LC and HC doses. In mice receiving combinations of suboptimal concentrations of calcitriol (VLC and LC) and suboptimal doses of letrozole or anastrozole (at 2.5 or 5 μg/mouse based on published observations [38, 39]), no significant changes were seen in serum calcium levels or body weights, demonstrating that the combination treatments were well tolerated.

Our earlier study showed enhanced inhibition of the growth of cultured MCF-7 cells when calcitriol was combined with three different AIs [14]. In this study, we sought to investigate whether calcitriol would enhance AI activity in vivo to inhibit the growth of MCF-7 tumor xenografts. It is clear that the selected suboptimal doses of calcitriol and the AIs exerted potent tumor inhibitory effects as single agents. Although the decreases in tumor volume due to the calcitriol–AI combinations achieved statistical significance when compared to the decreases caused by any of the single agents, the combinations at the doses tested did not exhibit noteworthy additive or synergistic effects in retarding tumor growth. It is possible that a longer treatment period or a finer dose response analysis might reveal a greater cooperative effect of the combined agents. Unlike the cell culture system, extensive dose response evaluation in mice was impractical. However, in gene expression studies, the combinations displayed additive and synergistic effects to modulate tumor gene expression appropriately.

Changes in aromatase expression in the various tissues also demonstrated the tissue selectivity of aromatase regulation by calcitriol in the mouse. It is now apparent that the organization of the aromatase gene in the mouse is more similar to the human aromatase gene than previously thought and the presence of exon I.3, I.4, and PII-derived transcripts seen in BCa cells have also been documented in various mouse tissues [26, 40]. As expected calcitriol administration reduced total aromatase mRNA levels in the human xenograft tumors. Our data now demonstrate differential regulation of aromatase by calcitriol in mouse tissues as well. Following calcitriol administration, aromatase mRNA expression levels remained unchanged in the uteri and ovaries and were increased in the bone marrow cells in intact mice. In contrast, the levels were decreased in the mammary adipose tissue of both intact and OVX mice.

Since we could not isolate adequate RNA from the highly mineralized adult bones, we examined the bone marrow cells that could be flushed from the femur. The data clearly show differential regulation of aromatase activity with an increase in aromatase mRNA levels in the bone marrow cells. In examining estrogen effects on bone, several published studies have used isolated bone marrow cells [41, 42], which contain many different cell populations including B and T lymphocytes, megakaryocytes, as well as endosteal and trabecular lining cells and mesenchymal stem cells (hMSCs) capable of differentiation along the osteogenic, chondrogenic, adipogenic, and marrow stromal lineages. In OVX mice estrogen treatment induced similar increases in ERE-luciferase reporter activity in both cortical bone and bone marrow-derived cells [42]. Hematopoetic lineage-negative cells from bone marrow have a population of osteoprogenitor cells that mineralize in vitro,

form bone in vivo and express bone-related genes [43, 44]. Further, calcitriol increases aromatase activity during osteogenic differentiation of the multipotent bone marrow-derived hMSCs [45]. Based on these observations, we used bone marrow cells in our study and aromatase mRNA level was up-regulated in these cells following calcitriol treatment. Thus, the pattern of aromatase regulation by calcitriol in mouse tissues is very similar to the pattern we have previously shown using human cell culture models [14] demonstrating that calcitriol exhibits SAM activity in vivo.

Mammary adipose tissue plays a vital role in defining the microenvironment for BCa and contributes significantly to BCa growth [7, 46, 47]. In BCa patients, the highest levels of aromatase transcripts have been found in the adipose tissue from the breast quadrants bearing tumors [48, 49]. Similar to these observations we detected an elevated expression of aromatase in the tumor-adjacent mammary adipose tissue compared to adipose tissue from mammary fat pads not bearing tumors. This elevation in aromatase expression is ascribed to a stimulation of aromatase transcription [7, 50–52] by tumor-derived proinflammatory factors such as prostaglandins (PGs) and cytokines [7, 53]. Calcitriol administration also significantly reduced aromatase mRNA levels in mammary tissue adjacent to BCa. This is likely due both to a direct repression of aromatase transcription as well as its anti-inflammatory action to reduce the production by the tumor of proinflammatory factors such as PGs [14] and the inhibition of the signaling pathways that they activate [9, 10]. This postulate is supported by the observation that calcitriol reduced the mRNA expression of COX-2, the key enzyme catalyzing PG synthesis, in the tumors from both intact and OVX mice.

Real-time RT-PCR and IHC data showed significant decreases in tumor aromatase and ERα expression at the mRNA and protein levels, respectively, following calcitriol treatment. These observations demonstrate that calcitriol inhibits both estrogen synthesis and signaling thereby reducing the major mitogenic signal provided by estrogens to promote BCa progression. Surprisingly, treatment with the enzyme inhibitors anastrozole or letrozole as single agents also produced significant decreases in aromatase but not ERα mRNA. Estrogens have been shown to exert a positive feed back regulation of aromatase transcription [54]. Therefore, the reduction in the levels of estrogens by AIs and the resultant attenuation of the feed back amplification of aromatase transcription might contribute to the observed reduction in aromatase mRNA following AI treatment. Our data in the postmenopausal model revealed decreases in intratumoral and mammary adipose E_1 and E_2 levels demonstrating the inhibition of aromatase activity and the blockade of estrogen synthesis following calcitriol

and letrozole treatments as single agents. The combination of these agents, which act by different mechanisms, produced the lowest E_1 and E_2 levels demonstrating cooperativity between calcitriol, a transcriptional repressor of aromatase and letrozole, an inhibitor of aromatase enzymatic activity. 17β-HSD1, the reductive isoform of the enzyme converts E_1 to E_2 in several tissues including BCa cells [55, 56]. Since the treatments did not change 17β-HSD1 mRNA levels in tumors and surrounding mammary fat, the observed decreases in E_2 levels were probably a consequence of reduced E_1 levels following the suppression of aromatase expression by the treatments.

Calcitriol regulation of tumor expression of genes that play key roles in inflammation, growth control and apoptosis were consistent with its tumor inhibitory activity. Calcitriol significantly suppressed the expression of the proinflammatory gene COX-2, demonstrating its anti-inflammatory activity. COX-2-derived PGE_2 is a major stimulator of aromatase transcription in BCa [7] and in tumor specimens from BCa patients aromatase expression strongly correlates with COX-2 expression [57]. Thus, suppression of COX-2 is an additional mechanism by which calcitriol decreases aromatase expression [18]. Treatment with AIs as single agents also reduced COX-2 mRNA and their combinations with calcitriol produced the greatest reduction in COX-2 expression. Calcitriol increased the mRNA levels of the cyclin-dependent kinase inhibitor p21/WAF1, whose expression is associated with G_0/G_1 cell cycle arrest and IGFBP-3, which has been shown to play an important role in calcitriol-mediated growth inhibition of malignant cells [58]. Again, its combination with an AI revealed a synergistic increase in IGFBP-3 mRNA. In general, cotreatment with an AI enhanced the regulatory effects of calcitriol on the expression of its key target genes, many of which (ERα, p21, IGFBP-3) were not altered by AI alone. Anastozole and letrozole, the two AIs used in our study, are both azole compounds, which are general inhibitors of cytochrome p450 enzymes. Several azole compounds such as ketoconazole and liarazole have been shown to inhibit 25-hydroxyvitamin D_3-24-hydroxylase (CYP24 A1), the enzyme that initiates the catabolism of calcitriol thereby extending the half-life of calcitriol and enhancing its biological activities [59–62]. It is possible that anastrozole and letrozole in addition to inhibiting aromatase (CYP19) also inhibit CYP24, a mechanism that could explain the enhancement of calcitriol effect on gene expression when combined with one of these AIs.

In conclusion, our data validate our cell culture observations (14) and demonstrate that calcitriol acts as a SAM in vivo. Calcitriol selectively decreased aromatase expression in the xenograft tumors and the surrounding mammary adipose tissue leading to a significant reduction

in estrogen synthesis, while having no effect on some tissues (ovary and uterus) and a stimulatory effect on other tissues (bone marrow cells). The different mechanisms of aromatase regulation due to calcitriol (suppression of aromatase transcription) and the AIs (inhibition of aromatase enzyme activity) were complementary, with the combination causing maximal inhibition of estrogen synthesis in the tumor microenvironment as reflected by the estrogen levels measured in the tumors and surrounding mammary fat. Calcitriol also inhibited estrogen signaling by decreasing ERα levels in the tumors and suppressed other inflammatory and growth signaling pathways [9, 10, 13]. At the selected doses, calcitriol and the AIs exhibited potent tumor inhibitory effects as single agents causing equivalent decreases in tumor volumes. Although we could not demonstrate the additivity of the combinations at these doses in terms of retardation of tumor growth, the combinations did exhibit additive and synergistic effects to appropriately regulate tumor gene expression reflecting cooperative anticancer activity. Cumulatively these actions would contribute to the beneficial effect of combining calcitriol with an AI to treat BCa. Furthermore, estrogen deprivation induced by AI treatment in bone increases the risk of BCa patients developing osteoporosis [5, 6]. Calcitriol, acting as a SAM to increase estrogen synthesis in bone (14) while reducing it in the breast, has the potential to ameliorate the AI-induced side effect of osteoporosis. Thus, we hypothesize that combining calcitriol with an AI would be a beneficial therapeutic approach in women with BCa.

Conflict of Interest The authors declare that they have no conflict of interest.

References

1. Goss P, Wu M (2007) Application of aromatase inhibitors in endocrine responsive breast cancers. Breast 16(Suppl 2):S114–S119
2. Riemsma R, Forbes CA, Kessels A, Lykopoulos K, Amonkar MM, Rea DW, Kleijnen J (2010) Systematic review of aromatase inhibitors in the first-line treatment for hormone sensitive advanced or metastatic breast cancer. Breast Cancer Res Treat 123:9–24
3. Rugo HS (2008) The breast cancer continuum in hormone-receptor-positive breast cancer in postmenopausal women: evolving management options focusing on aromatase inhibitors. Ann Oncol 19:16–27
4. Geisler J, Lonning PE (2005) Aromatase inhibition: translation into a successful therapeutic approach. Clin Cancer Res 11:2809–2821
5. Confavreux CB, Fontana A, Guastalla JP, Munoz F, Brun J, Delmas PD (2007) Estrogen-dependent increase in bone turnover and bone loss in postmenopausal women with breast cancer treated with anastrozole. Prevention with bisphosphonates. Bone 41:346–352
6. Mincey BA, Duh MS, Thomas SK, Moyneur E, Marynchencko M, Boyce SP, Mallett D, Perez EA (2006) Risk of cancer treatment-associated bone loss and fractures among women with breast cancer receiving aromatase inhibitors. Clin Breast Cancer 7:127–132
7. Simpson ER, Clyne C, Rubin G, Boon WC, Robertson K, Britt K, Speed C, Jones M (2002) Aromatase—a brief overview. Annu Rev Physiol 64:93–127
8. Gombart AF, Luong QT, Koeffler HP (2006) Vitamin D compounds: activity against microbes and cancer. Anticancer Res 26:2531–2542
9. Krishnan AV, Feldman D (2010) Molecular pathways mediating the anti-inflammatory effects of calcitriol: implications for prostate cancer chemoprevention and treatment. Endocr Relat Cancer 17:R19–R38
10. Krishnan AV, Feldman D (2010) Mechanisms of the anti-cancer and anti-inflammatory actions of vitamin D. Annu Rev Pharmacol Toxicol
11. Krishnan AV, Trump DL, Johnson CS, Feldman D (2010) The role of vitamin D in cancer prevention and treatment. Endocrinol Metab Clin North Am 39:401–418, table of contents
12. Trump DL, Deeb KK, Johnson CS (2010) Vitamin D: considerations in the continued development as an agent for cancer prevention and therapy. Cancer J 16:1–9
13. Welsh J (2007) Targets of vitamin D receptor signaling in the mammary gland. J Bone Miner Res 22(Suppl 2):V86–V90
14. Krishnan AV, Swami S, Peng L, Wang J, Moreno J, Feldman D (2010) Tissue-selective regulation of aromatase expression by calcitriol: implications for breast cancer therapy. Endocrinology 151:32–42
15. Simboli-Campbell M, Narvaez CJ, van Weelden K, Tenniswood M, Welsh J (1997) Comparative effects of 1,25(OH)$_2$D$_3$ and EB1089 on cell cycle kinetics and apoptosis in MCF-7 breast cancer cells. Breast Cancer Res Treat 42:31–41
16. Stoica A, Saceda M, Fakhro A, Solomon HB, Fenster BD, Martin MB (1999) Regulation of estrogen receptor-alpha gene expression by 1,25-dihydroxyvitamin D in MCF-7 cells. J Cell Biochem 75:640–651
17. Swami S, Krishnan AV, Feldman D (2000) 1alpha,25-Dihydroxyvitamin D$_3$ down-regulates estrogen receptor abundance and suppresses estrogen actions in MCF-7 human breast cancer cells. Clin Cancer Res 6:3371–3379
18. Krishnan AV, Swami S, Feldman D (2010) Vitamin D and breast cancer: inhibition of estrogen synthesis and signaling. J Steroid Biochem Mol Biol 121:343–348
19. Klein KA, Reiter RE, Redula J, Moradi H, Zhu XL, Brothman AR, Lamb DJ, Marcelli M, Belldegrun A, Witte ON, Sawyers CL (1997) Progression of metastatic human prostate cancer to androgen independence in immunodeficient SCID mice. Nat Med 3:402–408
20. Hershberger PA, Modzelewski RA, Shurin ZR, Rueger RM, Trump DL, Johnson CS (1999) 1,25-Dihydroxycholecalciferol (1,25-D$_3$) inhibits the growth of squamous cell carcinoma and down-modulates p21(Waf1/Cip1) in vitro and in vivo. Cancer Res 59:2644–2649
21. Hershberger PA, Yu WD, Modzelewski RA, Rueger RM, Johnson CS, Trump DL (2001) Calcitriol (1,25-dihydroxycholecalciferol) enhances paclitaxel antitumor activity in vitro and in vivo and accelerates paclitaxel-induced apoptosis. Clin Cancer Res 7:1043–1051
22. Koshizuka K, Koike M, Asou H, Cho SK, Stephen T, Rude RK, Binderup L, Uskokovic M, Koeffler HP (1999) Combined effect of vitamin D$_3$ analogs and paclitaxel on the growth of MCF-7 breast cancer cells in vivo. Breast Cancer Res Treat 53:113–120

23. Moreno J, Krishnan AV, Swami S, Nonn L, Peehl DM, Feldman D (2005) Regulation of prostaglandin metabolism by calcitriol attenuates growth stimulation in prostate cancer cells. Cancer Res 65:7917–7925

24. Livak KJ, Schmittgen TD (2001) Analysis of relative gene expression data using real-time quantitative PCR and the 2(−Delta Delta C(T)) method. Methods 25:402–408

25. Diaz-Cruz ES, Shapiro CL, Brueggemeier RW (2005) Cyclooxygenase inhibitors suppress aromatase expression and activity in breast cancer cells. J Clin Endocrinol Metab 90:2563–2570

26. Zhao H, Innes J, Brooks DC, Reierstad S, Yilmaz MB, Lin Z, Bulun SE (2009) A novel promoter controls Cyp19a1 gene expression in mouse adipose tissue. Reprod Biol Endocrinol 7:37

27. Zhao XY, Ly LH, Peehl DM, Feldman D (1999) Induction of androgen receptor by 1alpha,25-dihydroxyvitamin D₃ and 9-cis retinoic acid in LNCaP human prostate cancer cells. Endocrinology 140:1205–1212

28. Bradford MM (1976) A rapid and sensitive method for the quantitation of microgram quantities of protein utilizing the principle of protein dye binding. Anal Biochem 72:248–254

29. Allred DC, Carlson RW, Berry DA, Burstein HJ, Edge SB, Goldstein LJ, Gown A, Hammond ME, Iglehart JD, Moench S, Pierce LJ, Ravdin P, Schnitt SJ, Wolff AC (2009) NCCN Task Force Report: estrogen receptor and progesterone receptor testing in breast cancer by immunohistochemistry. J Natl Compr Canc Netw 7(Suppl 6):S1–S21, quiz S22–S23

30. Colston KW, Mackay AG, James SY, Binderup L, Chander S, Coombes RC (1992) EB1089: a new vitamin D analogue that inhibits the growth of breast cancer cells in vivo and in vitro. Biochem Pharmacol 44:2273–2280

31. Flanagan L, Packman K, Juba B, O'Neill S, Tenniswood M, Welsh J (2003) Efficacy of Vitamin D compounds to modulate estrogen receptor negative breast cancer growth and invasion. J Steroid Biochem Mol Biol 84:181–192

32. VanWeelden K, Flanagan L, Binderup L, Tenniswood M, Welsh J (1998) Apoptotic regression of MCF-7 xenografts in nude mice treated with the vitamin D₃ analog, EB1089. Endocrinology 139:2102–2110

33. Zinser GM, Tribble E, Valrance M, Urben CM, Knutson JC, Mazess RB, Strugnell SA, Welsh J (2005) 1,24(S)-dihydroxyvitamin D₂, an endogenous vitamin D₂ metabolite, inhibits growth of breast cancer cells and tumors. Anticancer Res 25:235–241

34. Jordan VC, Gottardis MM, Robinson SP, Friedl A (1989) Immune-deficient animals to study "hormone-dependent" breast and endometrial cancer. J Steroid Biochem 34:169–176

35. Robinson SP, Jordan VC (1989) Antiestrogenic action of toremifene on hormone-dependent, -independent, and heterogeneous breast tumor growth in the athymic mouse. Cancer Res 49:1758–1762

36. Santen RJ, Martel J, Hoagland M, Naftolin F, Roa L, Harada N, Hafer L, Zaino R, Pauley R, Santner S (1998) Demonstration of aromatase activity and its regulation in breast tumor and benign breast fibroblasts. Breast Cancer Res Treat 49(Suppl 1):S93–99, discussion S109–S119

37. Purohit A, Tutill HJ, Day JM, Chander SK, Lawrence HR, Allan GM, Fischer DS, Vicker N, Newman SP, Potter BV, Reed MJ (2006) The regulation and inhibition of 17beta-hydroxysteroid dehydrogenase in breast cancer. Mol Cell Endocrinol 248:199–203

38. Brodie A, Jelovac D, Macedo L, Sabnis G, Tilghman S, Goloubeva O (2005) Therapeutic observations in MCF-7 aromatase xenografts. Clin Cancer Res 11:884s–888s

39. Brodie A, Jelovac D, Sabnis G, Long B, Macedo L, Goloubeva O (2005) Model systems: mechanisms involved in the loss of sensitivity to letrozole. J Steroid Biochem Mol Biol 95:41–48

40. Chow JD, Simpson ER, Boon WC (2009) Alternative 5′-untranslated first exons of the mouse Cyp19A1 (aromatase) gene. J Steroid Biochem Mol Biol 115:115–125

41. Somjen D, Kaye AM, Harell A, Weisman Y (1989) Modulation by vitamin D status of the responsiveness of rat bone to gonadal steroids. Endocrinology 125:1870–1876

42. Windahl SH, Lagerquist MK, Andersson N, Jochems C, Kallkopf A, Hakansson C, Inzunza J, Gustafsson JA, van der Saag PT, Carlsten H, Pettersson K, Ohlsson C (2007) Identification of target cells for the genomic effects of estrogens in bone. Endocrinology 148:5688–5695

43. Itoh S, Aubin JE (2009) A novel purification method for multipotential skeletal stem cells. J Cell Biochem 108:368–377

44. Syed FA, Modder UI, Roforth M, Hensen I, Fraser DG, Peterson JM, Oursler MJ, Khosla S (2010) Effects of chronic estrogen treatment on modulating age-related bone loss in female mice. J Bone Miner Res 25:2438–2446

45. Pino AM, Rodriguez JM, Rios S, Astudillo P, Leiva L, Seitz G, Fernandez M, Rodriguez JP (2006) Aromatase activity of human mesenchymal stem cells is stimulated by early differentiation, vitamin D and leptin. J Endocrinol 191:715–725

46. Celis JE, Moreira JM, Cabezon T, Gromov P, Friis E, Rank F, Gromova I (2005) Identification of extracellular and intracellular signaling components of the mammary adipose tissue and its interstitial fluid in high risk breast cancer patients: toward dissecting the molecular circuitry of epithelial–adipocyte stromal cell interactions. Mol Cell Proteomics 4:492–522

47. Iyengar P, Espina V, Williams TW, Lin Y, Berry D, Jelicks LA, Lee H, Temple K, Graves R, Pollard J, Chopra N, Russell RG, Sasisekharan R, Trock BJ, Lippman M, Calvert VS, Petricoin EF 3rd, Liotta L, Dadachova E, Pestell RG, Lisanti MP, Bonaldo P, Scherer PE (2005) Adipocyte-derived collagen VI affects early mammary tumor progression in vivo, demonstrating a critical interaction in the tumor/stroma microenvironment. J Clin Invest 115:1163–1176

48. Bulun SE, Price TM, Aitken J, Mahendroo MS, Simpson ER (1993) A link between breast cancer and local estrogen biosynthesis suggested by quantification of breast adipose tissue aromatase cytochrome P450 transcripts using competitive polymerase chain reaction after reverse transcription. J Clin Endocrinol Metab 77:1622–1628

49. O'Neill JS, Elton RA, Miller WR (1988) Aromatase activity in adipose tissue from breast quadrants: a link with tumour site. Br Med J (Clin Res Ed) 296:741–743

50. Agarwal VR, Bulun SE, Leitch M, Rohrich R, Simpson ER (1996) Use of alternative promoters to express the aromatase cytochrome P450 (CYP19) gene in breast adipose tissues of cancer-free and breast cancer patients. J Clin Endocrinol Metab 81:3843–3849

51. Harada N (1997) Aberrant expression of aromatase in breast cancer tissues. J Steroid Biochem Mol Biol 61:175–184

52. Zhou C, Zhou D, Esteban J, Murai J, Siiteri PK, Wilczynski S, Chen S (1996) Aromatase gene expression and its exon I usage in human breast tumors. Detection of aromatase messenger RNA by reverse transcription-polymerase chain reaction. J Steroid Biochem Mol Biol 59:163–171

53. Meng L, Zhou J, Sasano H, Suzuki T, Zeitoun KM, Bulun SE (2001) Tumor necrosis factor alpha and interleukin 11 secreted by malignant breast epithelial cells inhibit adipocyte differentiation by selectively down-regulating CCAAT/enhancer binding protein alpha and peroxisome proliferator-activated receptor gamma: mechanism of desmoplastic reaction. Cancer Res 61:2250–2255

54. Kinoshita Y, Chen S (2003) Induction of aromatase (CYP19) expression in breast cancer cells through a nongenomic action of estrogen receptor alpha. Cancer Res 63:3546–3555

55. Laplante Y, Rancourt C, Poirier D (2009) Relative involvement of three 17beta-hydroxysteroid dehydrogenases (types 1, 7 and 12) in the formation of estradiol in various breast cancer cell lines using selective inhibitors. Mol Cell Endocrinol 301:146–153

56. Shields-Botella J, Chetrite G, Meschi S, Pasqualini JR (2005) Effect of nomegestrol acetate on estrogen biosynthesis and transformation in MCF-7 and T47-D breast cancer cells. J Steroid Biochem Mol Biol 93:1–13

57. Brodie AM, Lu Q, Long BJ, Fulton A, Chen T, Macpherson N, DeJong PC, Blankenstein MA, Nortier JW, Slee PH, van de Ven J, van Gorp JM, Elbers JR, Schipper ME, Blijham GH, Thijssen JH (2001) Aromatase and COX-2 expression in human breast cancers. J Steroid Biochem Mol Biol 79:41–47

58. Boyle BJ, Zhao XY, Cohen P, Feldman D (2001) Insulin-like growth factor binding protein-3 mediates 1 alpha,25-dihydrox-

yvitamin d(3) growth inhibition in the LNCaP prostate cancer cell line through p21/WAF1. J Urol 165:1319–1324

59. Feldman D (1986) Ketoconazole and other imidazole derivatives as inhibitors of steroidogenesis. Endocr Rev 7:409–420

60. Ly LH, Zhao XY, Holloway L, Feldman D (1999) Liarozole acts synergistically with 1alpha,25-dihydroxyvitamin D_3 to inhibit growth of DU 145 human prostate cancer cells by blocking 24-hydroxylase activity. Endocrinology 140:2071–2076

61. Muindi JR, Yu WD, Ma Y, Engler KL, Kong RX, Trump DL, Johnson CS (2010) CYP24A1 inhibition enhances the antitumor activity of calcitriol. Endocrinology 151:4301–4312

62. Peehl DM, Seto E, Hsu JY, Feldman DB (2002) Preclinical activity of ketoconazole in combination with calcitriol or the vitamin D analogue EB 1089 in prostate cancer cells. J Urol 168:1583–1588